CrystEngComm

PAPER

View Article Online
View Journal | View Issue

Cite this: *CrystEngComm*, 2014, **16**, 1741

Control of crystal structures of fluorescent two-component supramolecular systems by varying substituents and their positions†

Yuki Tanaka,[a] Hideyuki Tabata,[b] Nobuo Tajima,[c] Reiko Kuroda[b] and Yoshitane Imai*[a]

Received 22nd October 2013,
Accepted 5th December 2013

DOI: 10.1039/c3ce42128g

www.rsc.org/crystengcomm

Although fluorescent, column-like supramolecular network structures were previously obtained by using 2-naphthalenecarboxylic acid and benzylamine or fluorobenzylamine, the use of chlorobenzylamine or bromobenzylamine results in column-like or 2D-layered network supramolecular structures, indicating that crystal structures can be controlled by altering the type and position of the substituent on the benzylamine component.

Introduction

In solid-state chemistry, the chemical and physical properties of organic materials depend on the packing arrangements of component organic molecules.[1] In other words, by changing the packing arrangements of component molecules, the chemical and physical properties of solid-state organic materials can be controlled without utilizing synthetic methods.

Recently, solid-state supramolecular organic fluorophores with two or more components have attracted attention because their optical properties can be easily controlled by simply modifying the component molecules.[2] We recently reported supramolecular organic fluorophores composed of 2-naphthalenecarboxylic acid (**1**) and benzylamine and of **1** and fluorobenzylamine.[3] These supramolecular organic fluorophores are composed of column-like network structures built by **1** and benzylamine or fluorobenzylamine.

In the field of solid-state chemistry, molecules containing different substituents may lead to unique and specific chemical and physical properties of the solid-state material due to changes in the crystal structure. Thus, we expect that by varying the substituent in the components of 2-naphthalenecarboxylic acid-based supramolecular organic fluorophores, the structures and optical properties of the resulting supramolecular complexes can be controlled. However, it is typically difficult to predict the crystal structures of novel two-component systems.

In this paper, we describe novel fluorescent supramolecular structures by combining **1** with six different benzylamine derivatives (Chart 1). Specifically, we investigate the effects of substituents and substituent position in benzylamine derivatives on crystal structures and solid-state optical properties of two-component supramolecular systems. In this study, four halogen-containing benzylamine derivatives were investigated: 2-chlorobenzylamine (**2**), 3-chlorobenzylamine (**3**), 2-bromobenzylamine (**4**), and 3-bromobenzylamine (**5**). In addition, two methyl-substituted benzylamine derivatives were also explored: 2-methylbenzylamine (**6**) and 3-methylbenzylamine (**7**). This study elucidates information concerning the design of novel two-component supramolecular organic fluorophores.

Experimental

General

Compounds **2**, **4**, **5**, and the crystallization solvent (methanol, MeOH) were purchased from Wako Pure Chemical Industry and used as received. This commercial solvent was used

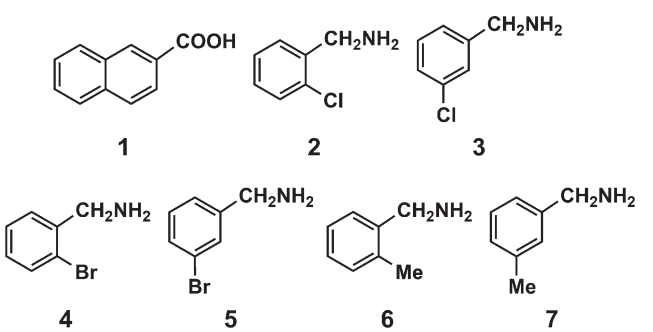

Chart 1

[a] *Department of Applied Chemistry, Faculty of Science and Engineering, Kinki University, 3-4-1 Kowakae, Higashi-Osaka, Osaka 577-8502, Japan. E-mail: y-imai@apch.kindai.ac.jp*
[b] *Research Institute for Science and Technology, Tokyo University of Science, 2641 Yamazaki, Noda-shi, Chiba, 278-8510, Japan*
[c] *First-Principles Simulation Group, Computational Materials Science Center, NIMS, Sengen, Tsukuba, Ibaraki 305-0047, Japan*

† CCDC 965542–965547. For crystallographic data in CIF or other electronic format see DOI: 10.1039/c3ce42128g

directly as obtained. Compounds **1**, **3**, **6**, and **7** were purchased from Tokyo Kasei Kogyo Co. and used as received.

Formation of complex by crystallization from solvent

Compounds **1** (10 mg, 5.8×10^{-5} mol) and **2** (or **3**–**7**, 5.8×10^{-5} mol) were dissolved in MeOH (3 mL) and left to stand at room temperature. After one week, a large number of crystals were obtained in all cases. The total weight of each crystal complex obtained in one batch was: complex **I** for the **1**–**2** system (8 mg); **II** for the **1**–**3** system (9 mg); **III** for the **1**–**4** system (7 mg); **IV** for the **1**–**5** system (9 mg); **V** for the **1**–**6** system (9 mg); and **VI** for the **1**–**7** system (8 mg).

X-ray crystallographic studies of crystals[4]

X-ray diffraction data for single crystals of **I**, **II**, and **IV** were collected using BRUKER APEX. X-ray diffraction data for single crystals of **III**, **V**, and **VI** were collected using RIGAKU SATURN 70R. The crystal structures were solved using the direct method[5] and refined by full-matrix least-squares using SHELX97.[5] The diagrams were prepared using PLATON.[6] Absorption corrections for **I**, **II**, and **IV** were performed using SADABS.[7] Absorption corrections for **III**, **V**, and **VI** were performed using multi-scan. Nonhydrogen atoms were refined with anisotropic displacement parameters, and hydrogen atoms were included in the models in their calculated positions in the riding model approximation.

Crystallographic data for I. $C_{11}H_8O_2{\cdot}C_7H_8ClN$, M = 313.77, monoclinic, space group $C2/c$, a = 18.671(2), b = 6.0403(6), c = 29.098(3) Å, β = 106.031(4)°, Z = 8, D_c = 1.322 g cm^{-3}, V = 3154.0(6) Å^3, μ(Mo Kα) = 0.248 mm^{-1}, 8452 reflections measured, 3107 unique reflections, final $R(F^2)$ = 0.0442 using 2667 reflections with $I > 2.0\sigma(I)$, R (all data) = 0.0511, T = 93(2) K. CCDC 965542.

Crystallographic data for II. $C_{11}H_8O_2{\cdot}C_7H_8ClN$, M = 313.77, orthorhombic, space group $Pbca$, a = 10.5204(7), b = 8.7184(6), c = 33.531(2) Å, Z = 8, D_c = 1.355 g cm^{-3}, V = 3075.5(3) Å^3, μ(Mo Kα) = 0.255 mm^{-1}, 17 697 reflections measured, 3610 unique reflections, final $R(F^2)$ = 0.0498 using 2827 reflections with $I > 2.0\sigma(I)$, R (all data) = 0.0647, T = 93(2) K. CCDC 965543.

Crystallographic data for III (ref. 8). $C_{11}H_8O_2{\cdot}C_7H_8BrN$, M = 358.23, triclinic, space group $P\bar{1}$, a = 4.6370(18), b = 11.658(4), c = 15.392(5) Å, α = 67.925(12)°, β = 82.161(15)°, γ = 85.996(18)°, Z = 2, D_c = 1.558 g cm^{-3}, V = 763.7(5) Å^3, μ(Mo Kα) = 2.698 mm^{-1}, 5471 reflections measured, 3268 unique reflections, final $R(F^2)$ = 0.0645 using 2811 reflections with $I > 2.0\sigma(I)$, R (all data) = 0.0757, T = 100(2) K. CCDC 965544.

Crystallographic data for IV. $C_{11}H_8O_2{\cdot}C_7H_8BrN$, M = 358.23, orthorhombic, space group $Pbca$, a = 10.6279(9), b = 8.7139(7), c = 33.989(3) Å, Z = 8, D_c = 1.512 g cm^{-3}, V = 3147.7(4) Å^3, μ(Mo Kα) = 2.618 mm^{-1}, 17 795 reflections measured, 3586 unique reflections, final $R(F^2)$ = 0.0524 using 2312 reflections with $I > 2.0\sigma(I)$, R (all data) = 0.0913, T = 93(2) K. CCDC 965545.

Crystallographic data for V (ref. 8). $C_{11}H_8O_2{\cdot}C_8H_{11}N$, M = 293.35, monoclinic, space group $C2/c$, a = 18.404(5), b = 6.0250(15), c = 28.832(8) Å, β = 104.628(3)°, Z = 8, D_c = 1.260 g cm^{-3}, V = 3093.4(14) Å^3, μ(Mo Kα) = 0.081 mm^{-1}, 7027 reflections measured, 3124 unique reflections, final $R(F^2)$ = 0.0537 using 1631 reflections with $I > 2.0\sigma(I)$, R (all data) = 0.1177, T = 100(2) K. CCDC 965546.

Crystallographic data for VI (ref. 8). $C_{11}H_8O_2{\cdot}C_8H_{11}N$, M = 293.35, monoclinic, space group $P2_1/c$, a = 15.604(4), b = 6.2630(14), c = 15.601(4) Å, β = 90.680(3)°, Z = 4, D_c = 1.278 g cm^{-3}, V = 1524.5(6) Å^3, μ(Mo Kα) = 0.083 mm^{-1}, 11 871 reflections measured, 4208 unique reflections, final $R(F^2)$ = 0.0433 using 3501 reflections with $I > 2.0\sigma(I)$, R (all data) = 0.0526, T = 100(2) K. CCDC 965547.

Measurement of X-ray powder diffraction (XRPD) spectra

X-ray powder diffraction (XRPD) patterns were recorded using a Rigaku MiniFlex II with graphite-monochromated CuKα radiation (30 kV, 15 mA). The spectra were measured at room temperature between 5° and 35° in the 2θ scan mode with a step size of 0.02° in 2θ and 40° min^{-1}.

Measurement of solid-state fluorescence spectra

Solid-state fluorescence spectra and absolute photoluminescence quantum yields were measured using an *Absolute PL Quantum Yield Measurement System (C9920-02, HAMAMATSU PHOTONICS K. K.)* under an air atmosphere at room temperature.

Results and discussion

The formation of fluorescent supramolecular systems was attempted *via* crystallization from MeOH. First, chlorine-containing supramolecular systems **1**–**2** and **1**–**3** were investigated. A mixture of **1** and **2** (or **3**) was dissolved in MeOH and left to stand at room temperature. After one week, a large number of colourless crystals **I** constructed from only **1** and **2** and colourless crystals **II** constructed from only **1** and **3** were obtained. Interestingly, although the previously reported **1**–2-fluorobenzylamine (or 3-fluorobenzylamine) supramolecular complex formed two types of crystal structures,[3] in this **1**–**2** (or **3**) system, only one type of crystal, **I** (or **II**), was formed. As the size of the substituent on the benzylamine component becomes larger, the difference in the stability of two polymorphic crystals becomes greater. Therefore, we hypothesize that when chlorine-containing compounds **2** and **3** were utilized in place of their corresponding fluorine-containing derivatives, only one type of crystal was formed.

X-ray crystallography was utilized in order to investigate the crystal structures of **I** and **II**. The crystal structures of **I** and **II** are shown in Fig. 1 and 2, respectively.

X-ray analysis revealed that the stoichiometry of **I** is **1** : **2** = 1 : 1, and the space group is $C2/c$. This complex has a column-like hydrogen- and ionic-bonded network structure along the b-axis (Fig. 1a and b). This column is formed by the carboxylate oxygen of the carboxylic acid anion in **1** (Fig. 1, indicated in blue) and the ammonium hydrogen of the protonated amine in **2** (Fig. 1, indicated in green). The complex is formed

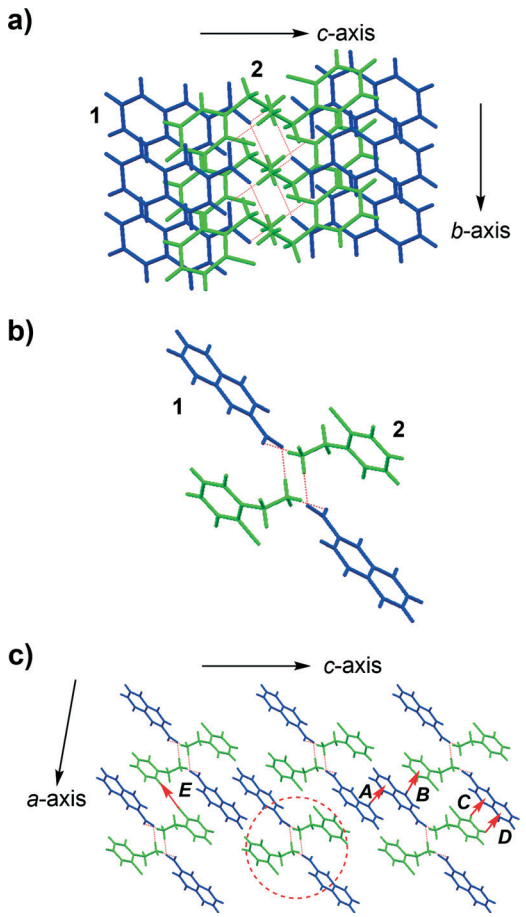

Fig. 1 Crystal structures of complex I. Components **1** and **2** are indicated in blue and green, respectively. (a) Columnar hydrogen-bonded and ionic-bonded network parallel to the *b*-axis. (b) View down the *b*-axis. (c) Packing structure observed along the *b*-axis. Solid red arrows A, B and C (or D) indicate intercolumnar naphthalene–naphthalene, naphthalene–benzene, and benzene–naphthalene edge-to-face interactions, respectively. The solid red arrow E indicates a halogen–halogen interaction. The red dotted circle indicates column-like network structure.

by the assembly of a column-like structure (represented by a red dotted circle in Fig. 1c). Each column interacts *via* intercolumnar naphthalene–naphthalene edge-to-face interactions between the hydrogen atoms of the naphthalene ring and the naphthalene ring in **1** [3.42 (C···π) Å, indicated by the solid red arrow A in Fig. 1c], naphthalene–benzene edge-to-face interactions between the hydrogen atoms of the naphthalene ring in **1** and the benzene ring in **2** [3.76 (C···π) Å, indicated by the solid red arrow B in Fig. 1c], two benzene–naphthalene edge-to-face interactions between the hydrogen atom of the benzene ring in **2** and the naphthalene ring in **1** [3.45 and 3.59 Å, indicated by the solid red arrows C and D in Fig. 1c], and a halogen–halogen interaction between the chlorine atoms of the benzene rings in **2** [3.42 (Cl···Cl) Å, indicated by the solid red arrow E in Fig. 1c].[9,10]

The crystal structure of **II** is shown in Fig. 2. Although the stoichiometry of **II** is also **1**:**3** = 1:1, the space group is *Pbca*. Interestingly, also in contrast to **I**, this crystal has a supramolecular 2D-layered hydrogen- and ionic-bonded network structure along the *a*- and *b*-axes (Fig. 2a and b). This 2D-layered network structure is formed by the carboxylate oxygen of the carboxylic acid anion in **1** (Fig. 2, indicated in blue) and the ammonium hydrogen of the protonated amine in **3** (Fig. 2, indicated in green). The 2D-layered network structure is maintained by intralayer naphthalene–naphthalene edge-to-face interactions between the hydrogen atoms of the naphthalene ring and the naphthalene ring in **1** [3.58 (C···π) Å, indicated by the solid red arrow A in Fig. 2a] and CH–π interactions between the hydrogen atom of the methylamine group and the benzene ring in **3** [3.59 (C···π) Å, indicated by the solid red arrow B in Fig. 2a].[9,10] The self-assembly of this 2D-layered network structure (represented by a red dotted border in Fig. 2c) with CCl–π (lone pair–π) interactions between the chlorine atom in **3** and the naphthalene ring in **1** [3.59 (Cl···π) Å, indicated by the solid purple arrow C in Fig. 2c] along the *c*-axis results in the formation of **II** (Fig. 2c).[9,10] These results suggest that in two-component

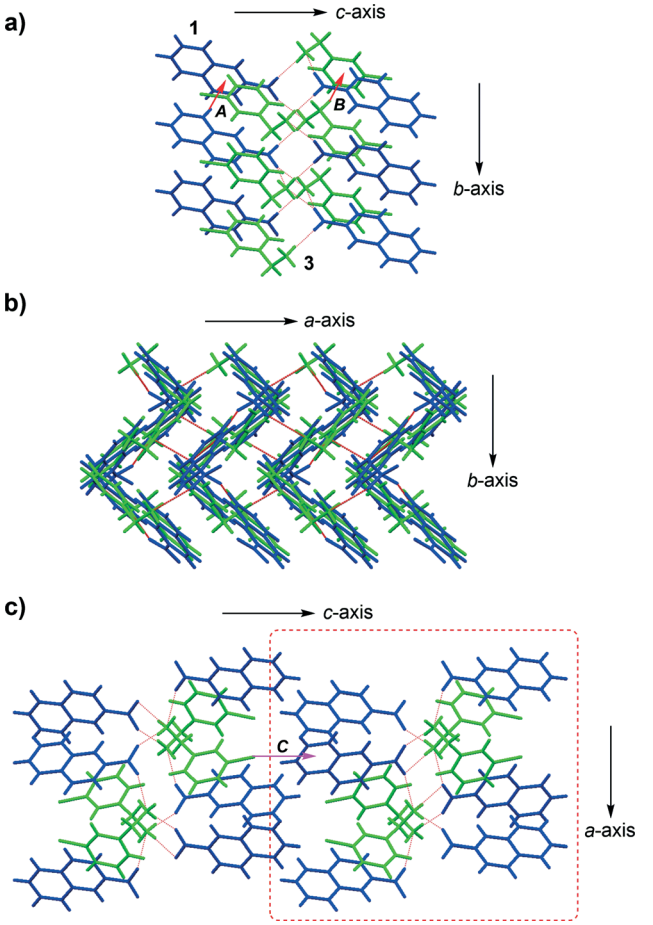

Fig. 2 Crystal structures of complex II. Components **1** and **3** are indicated in blue and green, respectively. (a) Extracted 2D-layered network structure observed along the *a*-axis. (b) View down the *c*-axis. (c) Packing structure comprising the 2D-layered network structure observed along the *b*-axis. Solid red arrows A and B show intralayer naphthalene–naphthalene edge-to-face and CH–π interactions, respectively. The solid purple arrow C indicates an interlayer CCl–π interaction. The red dotted border indicates the 2D-layered network structure.

supramolecular complexes containing 2-naphthalenecarboxylic acid and benzylamine derivatives, the substituent and its position on the benzylamine derivatives can dramatically alter the complexation behaviour and resulting crystal structures.

Next, preparation of supramolecular complexes containing bromobenzylamines **4** and **5** was attempted. Using the procedure described previously, a supramolecular complex was prepared *via* the complexation of **1** and **4** or **5**. In **1**–**4**- and **1**–**5**-systems, one type of complex, **III**, composed of **1** and **4**, and **IV**, composed of **1** and **5**, was obtained, respectively.

X-ray crystallography was utilized to analyze complexes **III** and **IV**. The crystal structure of **III** is shown in Fig. 3. The stoichiometry of **III** is **1**:**4** = 1:1, and the space group is $P\bar{1}$. Similar to **I**, complex **III** also has a column-like hydrogen- and ionic-bonded network structure composed of **1** (Fig. 3, indicated in blue) and **4** (Fig. 3, indicated in green) along the *a*-axis (Fig. 3a and b). In addition, this column-like structure is maintained by one intracolumnar CH–π interaction between the hydrogen atom of the methylamine group and the benzene ring in **4** [3.37 (C···π) Å, indicated by the solid red arrow A in Fig. 3a].[9,10] The self-assembly of this column-like structure (represented by a red dotted circle in Fig. 3c), without any major intercolumnar interactions, results in the formation of **III** (Fig. 3c).[9,10]

Comparison of **I** and **III** reveals the effect of substitution with chlorine *vs.* bromine. Although the organization of the column-like structures of **I** and **III** is similar, the orientation of their two component molecules is different (Fig. 1b and 3b). In addition, their packing styles are quite disparate (Fig. 1c and 3c). In **I**, the two neighbouring face-to-face naphthalene rings are independent when observed along the *b*-axis (Fig. 1c). On the other hand, the neighbouring face-to-face naphthalene rings in **III** are continuous when

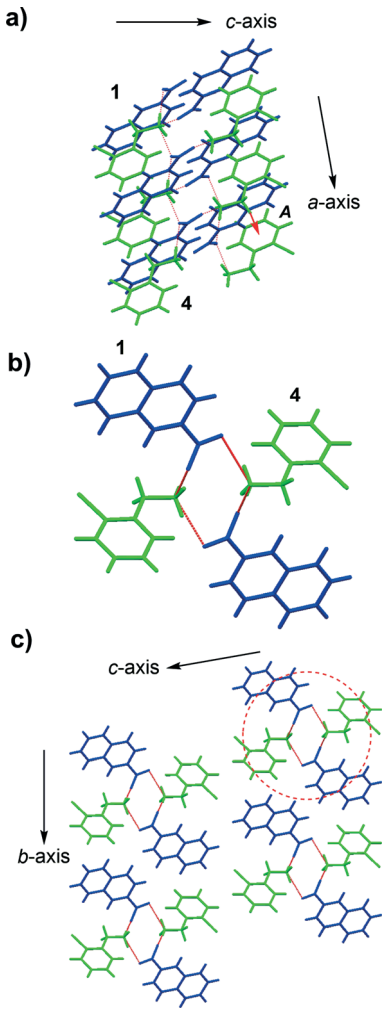

Fig. 3 Crystal structures of complex **III**. Components **1** and **4** are indicated in blue and green, respectively. (a) Columnar hydrogen-bonded and ionic-bonded network parallel to the *a*-axis. (b) View down the *a*-axis. (c) Packing structure observed along the *a*-axis. The solid red arrow A indicates an intracolumnar CH–π interaction. The red dotted circle indicates column-like network structure.

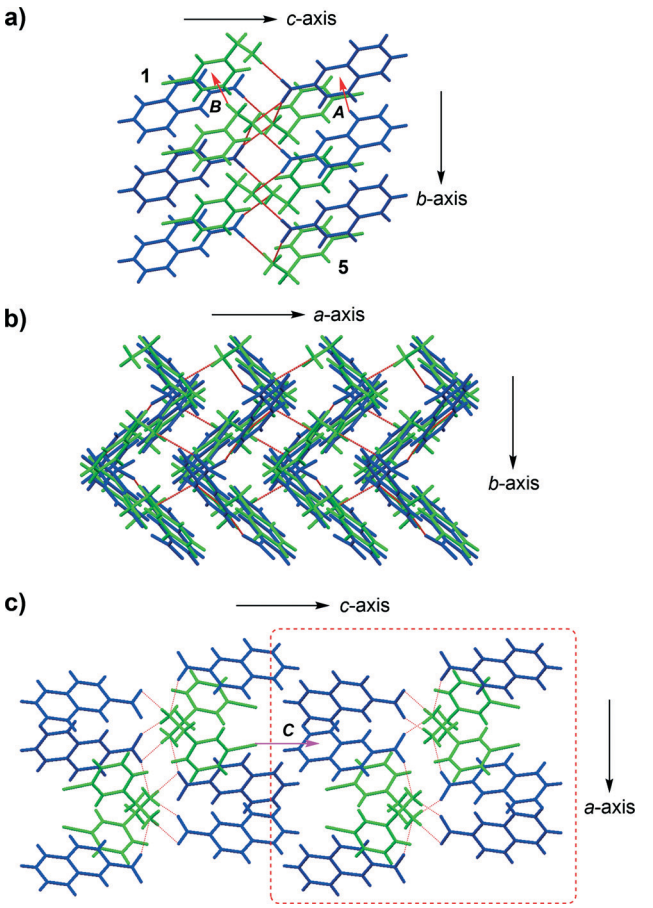

Fig. 4 Crystal structures of complex **IV**. Components **1** and **5** are indicated in blue and green, respectively. (a) Extracted 2D-layered network structure observed along the *a*-axis. (b) View down the *c*-axis. (c) Packing structure comprising the 2D-layered network structure observed along the *b*-axis. Solid red arrows A and B show intralayer naphthalene–naphthalene edge-to-face and CH–π interactions. The solid purple arrow C indicates an interlayer CBr–π interaction. The red dotted border indicates the 2D-layered network structure.

observed along the *a*-axis (Fig. 3c). Furthermore, the previously reported supramolecular complexes of **1**–2-fluorobenzylamine resulted in two types of complexes: a chiral complex and a complex with a 2 : 1 stoichiometry (**1** : 2-fluorobenzylamine).[3] This is in stark contrast to **I** and **III**, indicating that in 2-naphthalenecarboxylic acid-containing supramolecular complexes, the type of the substituent present on other components has a drastic effect on the complexation behaviour and crystal structures of the resulting complexes.

The crystal structure of **IV** is shown in Fig. 4. The previously reported **1**–3-fluorobenzylamine supramolecular system also has two types of complexes. One of the complexes is chiral and the stoichiometry of the other complex is **1** : 3-fluorobenzylamine = 2 : 1. The crystal structure of **IV** is quite different from that of the **1**–3-fluorobenzylamine complex, but it is identical to that of **II**. The stoichiometry of **IV** is **1** : **5** = 1 : 1 and the space group is *Pbca*. Compound **IV** also has a supramolecular 2D-layered hydrogen- and ionic-bonded network structure composed of **1** (Fig. 4, indicated in blue) and **5** (Fig. 4, indicated in green) maintained by intracolumnar naphthalene–naphthalene edge-to-face interactions between the hydrogen atoms of the naphthalene ring and the naphthalene ring in **1** [3.57 (C···π) Å, indicated by the solid red arrow A in Fig. 4a] and CH–π interactions between the hydrogen atom of the methylamine group and the benzene ring in **5** [3.57 (C···π) Å, indicated by the solid red arrow B in Fig. 4a] (Fig. 4a and b).[9,10] The self-assembly of this 2D-layered network structure (Fig. 4c, represented by a dotted red border) with CBr–π (lone pair–π) interactions between the bromine atom in **5** and the naphthalene ring in **1** [3.68 (Br···π) Å, indicated by the solid purple arrow C in Fig. 4c] along the *c*-axis results in the formation of **IV** (Fig. 4c).[9,10]

In order to investigate the bulk-formation behaviour of this supramolecular system, the X-ray powder diffraction (XRPD) patterns of bulk crystals obtained from solution were recorded in systems **1**–**2**, **1**–**3**, **1**–**4**, and **1**–**5** and compared to simulated XRPD patterns calculated from the crystal structure data (Fig. 5).

As a result, in all systems, the XRPD patterns of bulk crystals were the same as the simulated XRPD patterns calculated from the crystal structure data. This shows that one type of complex is obtained in systems **1**–**2**, **1**–**3**, **1**–**4**, and **1**–**5**.

Next, in order to further evaluate the effect of halogen-containing substituents on complexation behaviour, two methylbenzylamine derivatives, **6** and **7**, were investigated and compared to their halogen-containing benzylamine counterparts, **2**–**5**. Using the aforementioned procedure, a supramolecular complex was formed. In both **1**–**6**- and **1**–**7**-systems, one type of complex for each system was obtained and is denoted as **V** and **VI**, respectively. The crystal structures of complexes **V** and **VI** are shown in Fig. 6 and 7.

The stoichiometries of complexes **V** and **VI** are identical: **1** : **6** (or **7**) = 1 : 1. However, the space groups for the two complexes are different: $C2/c$ for **V** and $P2_1/c$ for **VI**. Interestingly, both **V** and **VI** have a columnar hydrogen- and ionic-bonded network structure along the *b*-axis (Fig. 6a, b and 7a, b), although **VI** uses a *meta*-substituted benzylamine derivative. Specifically, the column-like network structure in **VI** is a 2_1-helical columnar network. In **V** and **VI**, although these column-like structures are primarily formed by the carboxylate

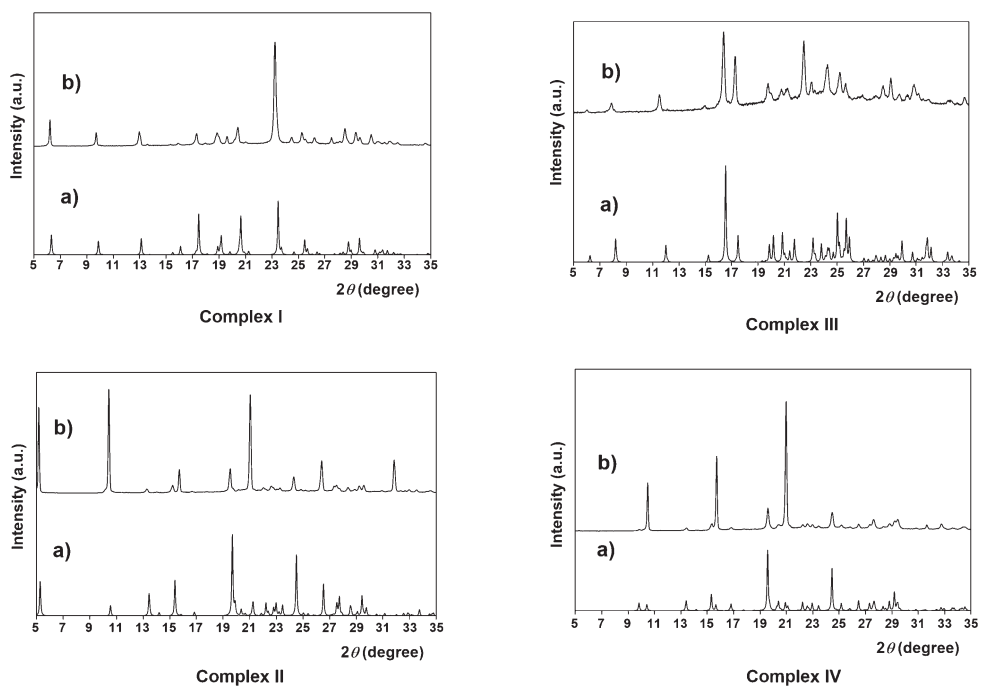

Fig. 5 X-ray powder diffraction (XRPD) patterns of complexes **I**–**IV**. (a) Simulated XRPD patterns of **I**–**IV** from crystal structure data and (b) XRPD patterns of complexes obtained by crystallization from solution.

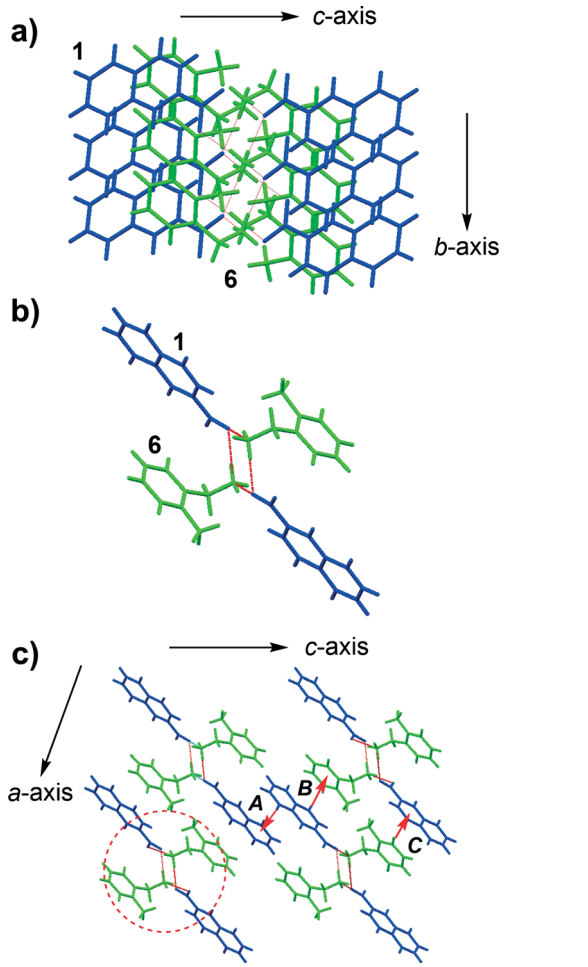

Fig. 6 Crystal structures of complex **V**. Components **1** and **6** are indicated in blue and green, respectively. (a) Columnar hydrogen-bonded and ionic-bonded network parallel to the *b*-axis. (b) View down the *b*-axis. (c) Packing structure observed along the *b*-axis. Solid red arrows A, B and C indicate intercolumnar naphthalene–naphthalene, naphthalene–benzene and benzene–naphthalene edge-to-face interactions, respectively. The red dotted circle indicates column-like network structure.

oxygen of the carboxylic acid anion in **1** (Fig. 6 and 7, indicated in blue) and the ammonium hydrogen of the protonated amine in **6** (or **7**) (Fig. 6 and 7, indicated in green), the 2_1-helical column structure in **VI** is also maintained by the intracolumnar naphthalene–benzene edge-to-face interactions between the hydrogen atom of the naphthalene ring in **1** and the benzene ring in **7** [3.61 (C⋯π) Å, indicated by the solid red arrow A in Fig. 7b] and CH–π interactions between the methyl group in **7** and the naphthalene ring in **1** [3.74 (C⋯π) Å, indicated by the solid red arrow B in Fig. 7b].[9,10]

Both complexes are formed by the assembly of these columns. In **V**, each column interacts *via* three intercolumnar interactions: (1) naphthalene–naphthalene edge-to-face interactions between the naphthalene rings in **1** [3.37 (C⋯π) Å, indicated by the solid red arrow A in Fig. 6c]; (2) naphthalene–benzene edge-to-face interactions between the hydrogen atoms of the naphthalene ring in **1** and the benzene ring in **6** [3.73 (C⋯π) Å, indicated by the solid red arrow B in Fig. 6c]; and (3) benzene–naphthalene edge-to-face interactions between the hydrogen atom of the benzene ring in **6** and the naphthalene ring in **1** [3.42 Å, indicated by the solid red arrow C in Fig. 6c].[9,10] On the other hand, in **VI**, each column interacts *via* intercolumnar naphthalene–naphthalene edge-to-face interactions between the naphthalene rings in **1** [3.40 (C⋯π) Å, indicated by the solid purple arrow C in Fig. 7c] and CH–π interactions between the hydrogen atom of the methylene group and the benzene ring in **7** [3.43 (C⋯…π) Å, indicated by the solid purple arrow D, Fig. 7c], and the hydrogen atom of the methylamine group and the benzene ring in **7**.[9,10] Although the packing style of **V** is different from that of **III**, it is similar

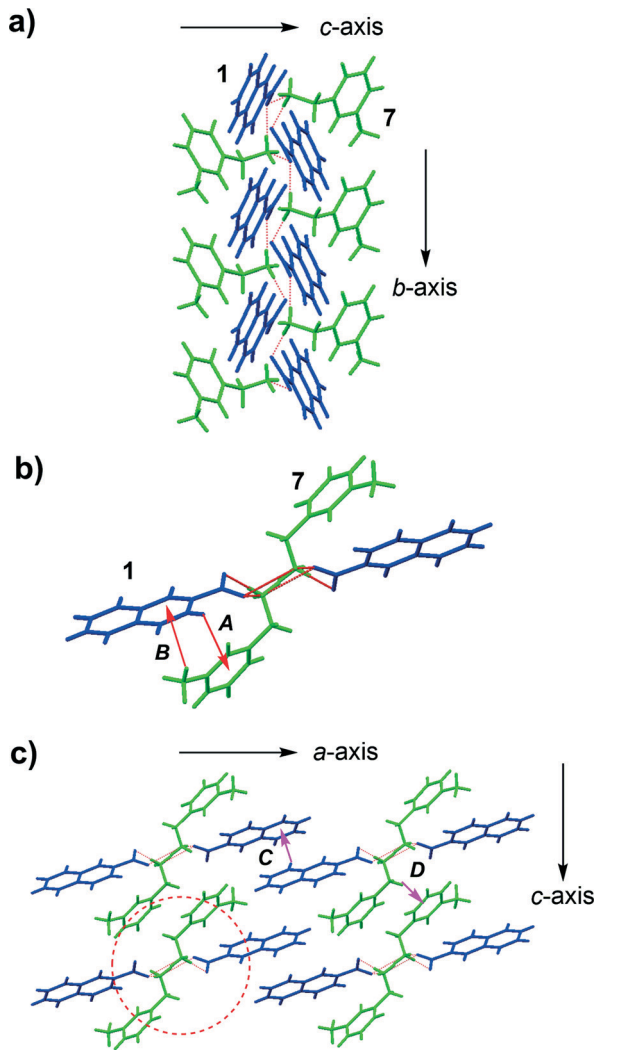

Fig. 7 Crystal structures of complex **VI**. Components **1** and **7** are indicated in blue and green, respectively. (a) Columnar hydrogen-bonded and ionic-bonded network parallel to the *b*-axis. (b) View down the *b*-axis. (c) Packing structure observed along the *b*-axis. Solid red arrows A and B indicate intracolumnar naphthalene–benzene edge-to-face and CH–π interactions, respectively. Solid purple arrows C and D indicate intercolumnar naphthalene–naphthalene edge-to-face and CH–π interactions, respectively. The red dotted circle indicates column-like network structure.

Table 1 Crystal form and solid-state fluorescence spectral data of complexes I–VI[a]

Complex	Crystal colour	Crystal shape	λ_{em}[a] nm^{-1}	Φ_F
I	Yellow	Block	348	0.12
II	Colourless	Plate	352	0.09
III	Colourless	Needle	ND	Weak
IV	Colourless	Plate	ND	Weak
V	Colourless	Block	350	0.28
VI	Colourless	Block	350	0.10

[a] Excitation wavelengths are 329, 339, 332, and 333 nm for complexes **I**, **II**, **V**, and **VI**, respectively.

to the packing style of **I**. On the other hand, the packing style of **VI** is different from that of both **I** and **III**. These results suggest that in 2-naphthalenecarboxylic acid-based supramolecular complexes, control of crystal structures may be influenced not only by the size of the substituent on the benzylamine derivative, but also by the halogen–π or CH–π interactions of the substituent on the benzylamine derivative.

To investigate the solid-state optical properties of the obtained supramolecular complexes **I–VI**, solid-state fluorescence spectra of these complexes were measured. The crystal form and solid-state fluorescence spectral data of **I–VI** are presented in Table 1. Although one important issue involving solid-state organic fluorophores is fluorescence quenching in the crystalline state, chlorine-containing complexes **I** and **II** and methyl-containing complexes **V** and **VI** exhibit fluorescence in the solid state. Bromine-containing complexes **III** and **IV** did not exhibit fluorescence. This is due to the heavy atom effect of bromine within the crystals. The solid-state fluorescence maxima (λ_{em}) in complexes **I**, **II**, **V**, and **VI** were not dramatically different. However, the absolute value of the photoluminescence quantum yield (Φ_F) increases in *ortho*-substituted complexes as compared to *meta*-substituted complexes. This might be explained by the lesser degree of interactions with neighbouring naphthalene units in the *ortho*-substituted complexes.

Conclusions

Two-component fluorescent supramolecular organic complexes were successfully created using **1** and chloro-, bromo-, or methyl-substituted benzylamine derivatives. Supramolecular complexes utilizing *ortho*-substituted, halogen-containing benzylamine derivatives are composed of column-like network structures. In contrast, supramolecular complexes employing *meta*-substituted, halogen-containing benzylamine derivatives are composed of 2D-layered network structures. These two types of crystal structures can be controlled by altering the substituent type and its position on the benzylamine component. In addition, 2-naphthalenecarboxylic acid-based supramolecular complexes show solid-state fluorescence when complexed with chlorobenzylamine or methylbenzylamine. These supramolecular systems are a substantial advancement in the development of novel solid-state organic fluorophores.

Acknowledgements

This study was supported by a Grant-in-Aid for Scientific Research (no. 24550165) from the Ministry of Education, Culture, Sports, Science and Development Program from JST and the KDDI Foundation.

Notes and references

1 (*a*) W. C. McCrone, *Physics and Chemistry of the Organic Solid State*, ed. D. Fox, M. M. Labes, A. Weissberger, Wiley Interscience, New York, 1965, vol. 2, pp. 725–767; (*b*) J. Bernstein, in *Organic Solid State Chemistry*, ed. G. R. Desiraju, Elsevier, Amsterdam, 1987, pp. 471–518; (*c*) J. D. Dunitz and J. Bernstein, *Acc. Chem. Res.*, 1995, **28**, 193–200; (*d*) N. Sanz, P. L. Baldeck, J. F. Nicoud, Y. L. Fur and A. Ibanez, *Solid State Sci.*, 2001, **3**, 867–875; (*e*) J. Bernstein, *Polymorphism in Molecular Crystals*, Clarendon, Oxford, 2002; (*f*) H. G. Brittain, *Polymorphism in Pharmaceutical Solids*, Marcel Dekker, Inc., New York, 1999; (*g*) L. Yu, *J. Phys. Chem. A*, 2002, **106**, 544–550; (*h*) P. Vishweshwar, J. A. McMahon, M. Oliveira, M. L. Peterson and M. J. Zaworotko, *J. Am. Chem. Soc.*, 2005, **127**, 16802–16803; (*i*) T. Mutai, H. Satou and K. Araki, *Nat. Mater.*, 2005, **4**, 685–687; (*j*) G. R. Desiraju, *Cryst. Growth Des.*, 2008, **8**, 3–5; (*k*) D. E. Braun, T. Gelbrich, R. K. R. Jetti, V. Kahlenberg, S. L. Price and U. Griesser, *Cryst. Growth Des.*, 2008, **8**, 1977–1989; (*l*) A. Brillante, I. Bilotti, R. Guido, D. Valle, E. Venuti and A. Girlando, *CrystEngComm*, 2008, **10**, 937–946; (*m*) J. Bernstein, J. D. Dunitz and A. Gavezzotti, *Cryst. Growth Des.*, 2008, **8**, 2011–2018; (*n*) Y. Imai, T. Kinuta, K. Nagasaki, T. Harada, T. Sato, N. Tajima, Y. Sasaki, R. Kuroda and Y. Matsubara, *CrystEngComm*, 2009, **11**, 1223–1226; (*o*) J. Tian, S. J. Dalgarno and J. L. Atwood, *J. Am. Chem. Soc.*, 2011, **133**, 1399–1404, and references cited therein.

2 (*a*) Y. Mizobe, N. Tohnai, M. Miyata and Y. Hasegawa, *Chem. Commun.*, 2005, 1839–1841; (*b*) S. Oshita and A. Matsumoto, *Langmuir*, 2006, **22**, 1943–1945; (*c*) Y. Ooyama and K. Yoshida, *Eur. J. Org. Chem.*, 2008, 2564–2570; (*d*) J. Luo, T. Lei, L. Wang, Y. Ma, Y. Cao, J. Wang and J. Pei, *J. Am. Chem. Soc.*, 2009, **131**, 2076–2077; (*e*) T. Kinuta, K. Kamon, T. Harada, Y. Nakano, N. Tajima, T. Sato, M. Fujiki, R. Kuroda, Y. Matsubara and Y. Imai, *Eur. J. Org. Chem.*, 2009, 5760–5764; (*f*) N. Nishiguchi, T. Sato, T. Kinuta, R. Kuroda, Y. Matsubara and Y. Imai, *Cryst. Growth Des.*, 2011, **11**, 827–831; (*g*) N. Nishiguchi, T. Kinuta, Y. Nakano, T. Harada, N. Tajima, T. Sato, M. Fujiki, R. Kuroda, Y. Matsubara and Y. Imai, *Chem.–Asian J.*, 2011, **6**, 1092–1098; (*h*) N. Nishiguchi, T. Kinuta, T. Sato, Y. Nakano, H. Tokutome, N. Tajima, M. Fujiki, R. Kuroda, Y. Matsubara and Y. Imai, *Chem.–Asian J.*, 2012, **7**, 360–366; (*i*) N. Taniguchi, R. Shimomaki, T. Amako, T. Sato, H. Tokutome, N. Tajima, R. Kuroda, M. Fujiki and Y. Imai, *Asian J. Org. Chem.*, 2013, **2**, 681–687.

3 (*a*) Y. Kobayashi, T. Kinuta, T. Sato, T. Harada, R. Kuroda, Y. Matsubara and Y. Imai, *CrystEngComm*, 2012, **14**, 1468–1472; (*b*) Y. Kobayashi, T. Sato, Y. Tanaka, T. Harada, R. Kuroda and Y. Imai, *CrystEngComm*, 2013, **15**, 4624–4630.
4 Crystallographic table of complexes **I–VI** is shown in Table ESI-1.†
5 G. M. Sheldrick, SHELXL97 *Acta Crystallogr., Sect. A: Found. Crystallogr.*, 2008, **64**, 112–122.
6 A. L. Spek, PLATON, *A Multipurpose Crystallographic Tool*, Utrecht University, Utrecht, Netherlands, 2010.
7 G. M. Sheldrick, SADABS, *Program for Empirical Absorption Correction of Area Detector Data*, University of Gottingen, Germany, 1996.
8 Sufficient diffraction intensities could not be obtained because the crystal size was too small.
9 It was determined using PLATON geometry calculation.
10 The details of interactions are shown in Table ESI-2–7.†

